J. Fluid Mech. (1970), *vol.* 40, *part* 1, *pp.* 39–47
Printed in Great Britain

Stability of time-dependent rotational Couette flow. Part 1. Experimental investigation

By R. P. KIRCHNER
Mechanical Engineering Department, Newark College of Engineering

AND C. F. CHEN
Department of Mechanical and Aerospace Engineering, Rutgers University

(Received 7 March 1969 and in revised form 20 June 1969)

The stability of viscous time-dependent rotational Couette flow, induced by an impulsively started inner cylinder was experimentally investigated. The ratio of the radius of the inner cylinder to that of the outer cylinder was $\frac{1}{10}$. The space between the cylinders was filled with distilled water. The time-dependent instabilities were observed by means of dye injection. They appeared as a series of disks more or less evenly spaced along the inner cylinder. The spacing and growth of these instabilities were recorded using a motion picture camera. From the motion pictures the critical time (which is the time from the impulsive start to the first onset of instability) and spacing of the instabilities were experimentally determined, and a marginal stability curve (Reynolds number *versus* critical time) was constructed.

1. Introduction

Many flows encountered in engineering practice and in nature are unsteady. To cite a few examples: the flow past a helicopter blade and the flow about an airplane penetrating a gust are unsteady; the flow of blood in the aorta is pulsatile; and geophysical flows are usually time-dependent. These unsteady flows, similar to the steady flows, have clearly defined régimes of laminar and turbulent motion with a transitional régime bridging the two. In steady flow, the linear stability theory predicts the critical Reynolds number beyond which infinitesimal disturbances will tend to grow. With the results of the linear theory as a point of departure, and through the use of non-linear analysis, a picture of the transitional process is beginning to emerge for certain flow situations. In unsteady flows, even the initial step of stability analysis has not been very well established. There are two reasons: (i) the experimental investigation is much more difficult than in the steady case; (ii) the criteria for stability cannot be uniquely stated as in the steady flow case. The former fact motivated us to design a simple experiment in which reliable data may be obtained on the instability of unsteady flow. The experiment chosen was that of a rotating Couette flow, in which the inner cylinder was impulsively started.

The stability of steady Couette flow has been the subject of both experimental and theoretical investigations by many authors, since Taylor (1923) first discovered the cellular secondary flow. Donnelly (1964) has reported that the onset of instability could be inhibited by modulating the rate of rotation of the inner cylinder. More recently, Chen & Christensen (1967) observed a Taylor-like instability in the time-dependent flow induced by an impulsively started rotating cylinder in a large tank of water. The present experiment is an outgrowth of this work.

In this paper we summarize the experimental results obtained in a wide-gap circular Couette flow apparatus. The inner cylinder, whose radius is one-tenth that of the outer cylinder, was impulsively started. The outer cylinder remained stationary. The flow was made visible by the admission of a neutral density dye solution through the inner cylinder, and the events were recorded by the use of a motion picture camera. In part 2 (Kirchner & Chen 1970), we shall discuss the theoretical methods of predicting the stability boundary of such a flow, and present the results of stability calculations based on the 'quasi-steady' and 'momentary stability' approaches. In what follows, the experimental apparatus and procedures are presented in an abbreviated form; more details may be found in Kirchner (1968). The initiation and growth of the instability, which appeared as a series of disks more or less evenly spaced along the inner cylinder, are illustrated by photographs printed from selected frames of the motion picture.† Finally, an experimental marginal stability curve is constructed.

2. Apparatus

The apparatus is shown schematically in figure 1. A $\frac{1}{2}$ in. cylinder was rotated concentrically in a 5 in. cylinder by means of a Graham variable speed drive. The inner cylinder consisted of a brass tube with a diameter of $0{\cdot}5007 \pm 0{\cdot}0002$ in., a length of $36\frac{1}{4}$ in., and a maximum runout of $\pm 0{\cdot}5$ % of the radius in a bearing length of 31 in. The cylinder was sealed at the top and bottom. A $\frac{1}{4}$ in. hole, drilled perpendicular to the cylinder axis and $1\frac{3}{8}$ in. from the top, provided the entrance for the dye solution through a stationary dye manifold. A centred slit 5 in. long, 0·014 in. wide and $\frac{1}{16}$ in. deep was cut longitudinally in the cylinder. Forty-one holes 0·0135 in. in diameter and spaced $\frac{1}{8}$ in. apart were drilled in the slit to permit dye injection. With this arrangement, we were able to spread the dye uniformly around the inner cylinder. The outer cylinder was a plexiglas tube with a diameter of $5 \pm \frac{1}{16}$ in. and a thickness of $\frac{1}{4}$ in. The diameter of the outer cylinder need not be precisely controlled, since the critical times we are encountering are approximately $\frac{1}{10}$ or less of the time needed to establish steady flow in the annulus. The cylindrical apparatus was constructed 30 in. long. This 30 in. length represents a compromise, in that the cylinder length must be short enough to maintain a reasonable runout for the inner cylinder, yet long enough to reduce end effects. Christensen (1966) experimentally checked the effects of

† This motion picture is listed as catalogue number K6, *Stability of Time-Dependent Rotational Couette Flow*, in the ASME-ESL Film Library. A copy of the film may be borrowed from the Engineering Societies Library, 345 E. 47th St, New York, N.Y. 10017.

two different end conditions on the critical time for a rotating cylinder in a water tank. One condition was the stationary end wall, and the other was the rotating end wall. He found essentially that the critical time was not affected.

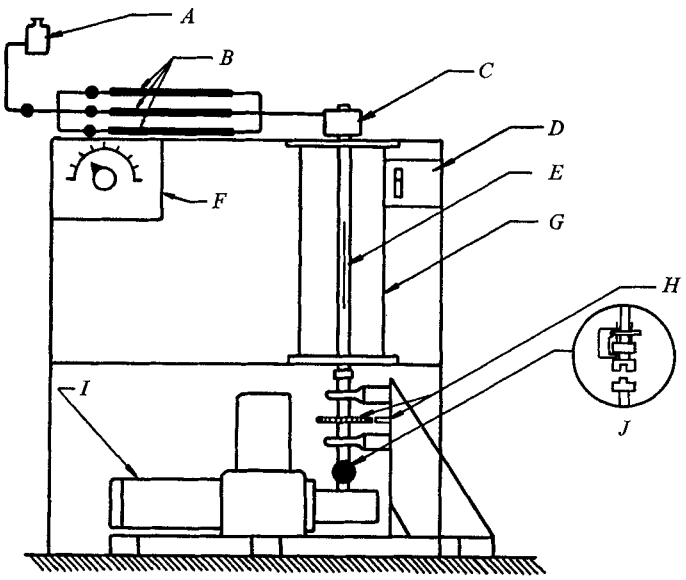

FIGURE 1. Experimental apparatus. *A* Dye reservoir. *B* Capillary tubes. *C* Dye manifold. *D* Clock. *E* $\frac{1}{2}$ in. O.D. shaft. *F* Jordan speed control. *G* 5 in. I.D. cylinder. *H* Gear and magnetic pickup. *I* Graham drive. *J* Clutch.

The speed of the rotating shaft was determined with a magnetic pickup and gear arrangement. A 96 tooth steel gear, with a pitch diameter of 3 in., was mounted on the drive shaft just above the clutch. The magnetic pick-up was mounted parallel to the gear with a clearance of 0·006 in. The output voltage frequency, which varied linearly with the speed, was measured on a Hewlett Packard electronic counter.

The inner cylinder was started impulsively by means of an interlocking clutch (see figure 1). The impulsive start was investigated in order to compare the actual speed-time behaviour with the ideal step function. The results showed that the start was very close to being a step function, but with a very small time lag. This time lag was less than 0·5 % of the shortest critical time observed. A Lab-Chron electric timer, which was mounted in the view of the camera, was activated by means of a limit switch when the clutch was engaged.

Nigrosine dye was used for flow visualization. Only a very small quantity of Nigrosine dye crystal (approximately 35 parts per million by weight) was needed to produce good flow visualization results. Before each test the density of the dye solution was checked by placing a drop in a beaker of undyed distilled water. When the drop neither rose nor fell, it was considered to be a neutral density solution.

3. Experimental procedure and results

The space between the cylinders was filled with distilled water. Then the water was drawn back through the dye injection system to the reservoir in order to purge the system of air. The system was allowed to settle for at least 8 h in order to permit disturbances to die out and the water to come to room temperature. The temperature of the water in the cylinder at six locations over the 30 in. height was recorded in order to check on temperature stratification. Considering the maximum error in the temperature measurement, the maximum stratification of ten tests was found to be 1° F over the 30 in. height. After the 8 h settling period, the Nigrosine dye was added to the water in the reservoir and the dye solution was tested and adjusted for neutral density. Next, the valves were opened, and the dye solution flowed slowly to the slit. As the dye flowed out of the slit the inner cylinder was rotated by hand in order to wipe the dye around the cylinder. Then the temperature was recorded. With the speed set at the proper test value the clutch was engaged. When the clutch engaged, the electric timer, one direct floodlight, and two indirect spotlights were turned on automatically. For tests with long critical times, the lights were turned on manually at a later time to avoid excessive heating of the fluid.

3.1. *Experimental observations*

A Cine-Kodak 16 mm movie camera was used to record the critical time and the growth of the instabilities. Selected frames from the film are shown in figure 2, plate 1, to illustrate the sequence of events from the start of rotation of the cylinder to the presence of toroidal vortices. First, the dye was injected, and the inner cylinder was slowly rotated by hand, in order to form a more or less uniform sheath of dye around the cylinder, as shown in (*a*). Then the inner cylinder was started impulsively to rotate at 26·9 rev/min or $R = 124$. The Reynolds number R is based on the surface speed and radius of the inner cylinder. The laminar motion before the onset of instability is shown in (*b*). At approximately 6·4 to 8·3 sec after the impulsive start, the flow became unstable. The start of the radial flow of the instability disks can be seen in (*c*). These disks grow as time increases, as shown in (*d*). The rim of each disk is curled inward on the top and bottom to form a set of toroidal vortices as shown in (*e*). A better picture of the toroidal vortices is shown in (*f*), which was taken from another test run at 25·6 rev/min or $R = 118$. It is of interest to note that the steady state critical Reynolds number for this apparatus ($\eta = 0{\cdot}10$) as given by Walowit, Tsao & Di Prima (1964) is 15·7. In this experiment, the critical Reynolds number ranged from 30·8 to 275.

Another set of four frames taken from a test conducted at 60·6 rev/min or $R = 275$ are shown in figure 3, plate 2. All four pictures were taken after the critical time of 1·9 sec. As compared with the pictures in figure 2 the spacing between the instability disks is smaller. The results show that as the Reynolds number increases the instability disk spacing decreases.

The motion pictures show that the system of toroidal vortices itself is unstable. After the disks form and grow as toroidal vortices, they undergo a complicated

interchange process whereby the initial number of toroidal vortices is reduced to a small number. The sketches in figure 4 show a frequently observed interaction between two toroidal vortices. Figure 4 (*a*) shows the system of toroidal vortices before the interchange process, in (*b*) an axial flow periodic in the axial direction begins to rotate the toroidal vortices, in (*c*) and (*d*) the distorted vortices begin to form a new toroidal vortex. Further details of the interchange process and the formation of the steady state flow from the initial system of vortices are currently under study.

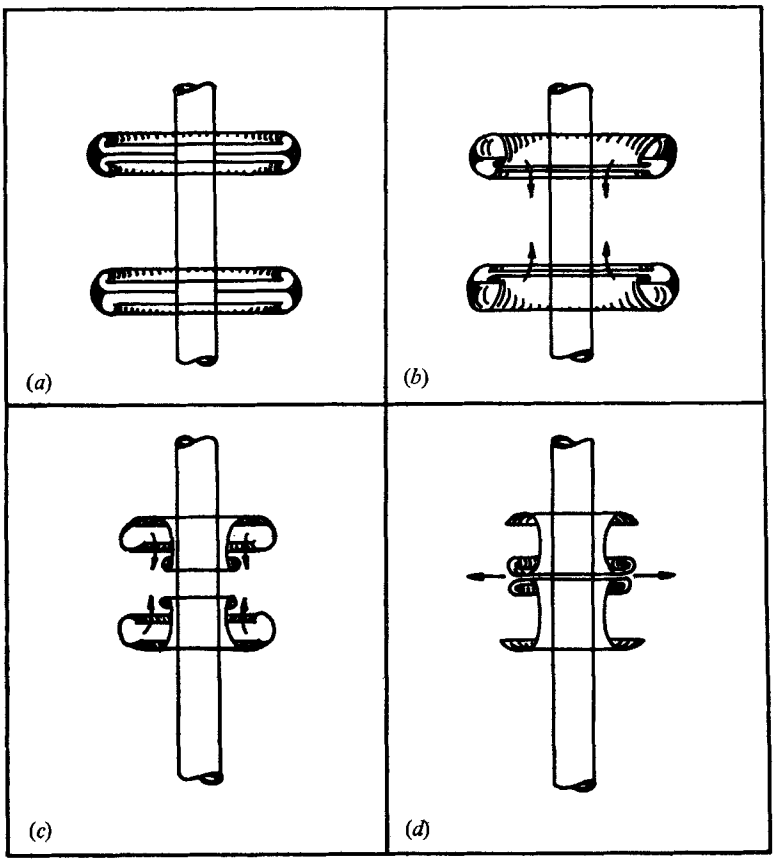

FIGURE 4. Sketch of vortex interchange at successive times ($t_a < t_b < t_c < t_d$).

3.2. *Data and discussion*

The motion pictures show that the dye spreads around the rotating cylinder in layers. In general, as time increases, these layers lose their stratified appearance and become one continuous sheath of dye around the cylinder. Then, the instability in the form of regularly spaced disks begins to form.

The critical time is the time at the onset of instability. In the transient Taylor stability problem, the critical time marks the first time when disturbances grow

faster than the basic flow. Any disturbance that grows considerably faster than the basic flow will be easily detected by the dye flow visualization technique. However, it may be difficult to detect the start of disturbances which grow only slightly faster than the basic flow. The experiments show that for $R > 100$ the instabilities grow very rapidly compared with the basic flow, and therefore the critical time can easily be determined from the motion pictures. The critical time was recorded as the time (considered zero at the impulsive start) from the first unstratification of the dye layers to the time when the instabilities were first clearly visible. Thus the critical time was determined by locating the last time of definite stability and the first time of definite instability.

In table 1, data collected from thirty test runs are presented. We have arbitrarily arranged the data in three groups according to Reynolds number: $R < 60$, $60 \leqslant R \leqslant 100$, $R > 100$. The high speed group has an average value for the dimensionless critical time period $\Delta\tau_c$ of 0·024; the medium speed group 0·071; and the low speed group of 0·14.

Convection currents, due to heating from the floodlight, were observed near the surface of the outer cylinder during tests of low Reynolds numbers (Reynolds numbers less than 60 and critical times exceeding 35 sec). At these low Reynolds numbers, the instabilities may also be affected by a slight axial flow, caused by not having the density of the dye solution exactly the same as that of the water. In addition, these instabilities form rather weakly, and may be affected by the end conditions. They do not seem to grow everywhere at once, as in the higher Reynolds number case, but seem to propagate from the ends of the cylinder toward the centre. These effects caused uncertainty in the critical time value, and can cause a significant spread of experimental data. In the range $60 \leqslant R \leqslant 100$ the instabilities form in approximately a regular manner, and grow more rapidly than in the $R < 60$ case. With the dye solution carefully adjusted for neutral density, quite reliable data can be obtained in this Reynolds number range. Above Reynolds numbers of approximately 100, the instabilities form very rapidly, and grow so strongly that the convection currents caused by the floodlights are negligible; even if the dye density is not exactly a neutral density solution, it does not seem to affect the critical time significantly. At these higher Reynolds numbers, if the instabilities are initiated at the ends of the cylinders, then they propagate so fast that they appear to grow in a regular manner everywhere at once.

The experimental results are shown in table 1, and a plot of Reynolds number *versus* dimensionless critical time is shown in figure 5 along with the experimental results of Chen & Christensen (1967). In general, the present data lie in the stable region of the data of Chen & Christensen. This may be attributed to the improved dye-injection system. With the present dye-injection system a better determination of the onset of instability can be made. The presence of the outer cylinder should not influence the results to any appreciable degree since at $\tau = 1$ basic flow velocity distributions are almost exactly the same for these two cases.

A series of five tests were run at $R = 160$ in order to spot check the reproducibility of the data. The results shown in table 1 and figure 5 are very good. An

Run no.	Temp. (° F)	Speed (r.p.m.)	Reynolds no.	Taylor† no.	Critical time (sec)	Dimensionless critical time $\left(\tau = \frac{\nu t}{R_1^2}\right)$
1	66·45	7·5	30·8	$0{\cdot}252 \times 10^6$	85·0–95·0	2·16–2·42
2	67·95	8·75	36·7	$0{\cdot}356 \times 10^6$	98·0–102·0	2·45–2·55
3	68·05	10·0	42·0	$0{\cdot}467 \times 10^6$	37·0–43·0	0·923–1·07
4	69·30	10·0	42·7	$0{\cdot}483 \times 10^6$	47·0–55·0	1·153–1·350
5	67·00	10·6	43·9	$0{\cdot}510 \times 10^6$	67·8–69·8	1·72–1·76
6	73·60	11·9	53·7	$0{\cdot}765 \times 10^6$	25·7–29·6	0·596–0·687
7	74·35	11·9	54·2	$0{\cdot}779 \times 10^6$	28·5–34·0	0·655–0·782
8	75·28	13·75	63·4	$1{\cdot}06 \times 10^6$	20·0–24·0	0·454–0·545
9	73·30	14·7	66·1	$1{\cdot}16 \times 10^6$	15·2–18·4	0·354–0·428
10	72·05	16·25	71·9	$1{\cdot}37 \times 10^6$	14·3–18·6	0·338–0·440
11	71·80	18·75	82·6	$1{\cdot}81 \times 10^6$	13·0–16·3	0·309–0·387
12	68·45	21·5	90·7	$2{\cdot}18 \times 10^6$	12·0–14·6	0·300–0·362
13	72·50	21·9	97·4	$2{\cdot}51 \times 10^6$	10·6–11·5	0·250–0·271
14	72·35	24·3	108	$3{\cdot}09 \times 10^6$	9·5	0·22
15	75·65	25·6	118	$3{\cdot}37 \times 10^6$	7·7–9·4	0·17–0·21
16	69·30	28·1	120	$3{\cdot}81 \times 10^6$	7·4–9·4	0·18–0·23
17	75·35	26·9	124	$4{\cdot}08 \times 10^6$	6·4–8·3	0·15–0·19
18	79·80	27·81	136	$4{\cdot}88 \times 10^6$	5·1–6·7	0·11–0·14
19	67·90	36·2	152	$6{\cdot}10 \times 10^6$	4·3–5·4	0·11–0·13
20	80·80	37·875	157	$6{\cdot}56 \times 10^6$	3·4–5·0	0·072–0·11
21	71·80	36·25	160	$6{\cdot}77 \times 10^6$	4·8–5·3	0·11–0·13
22	72·20	36·25	160	$6{\cdot}84 \times 10^6$	4·6–5·4	0·11–0·13
23	72·50	36·2	161	$6{\cdot}87 \times 10^6$	3·9–5·2	0·092–0·12
24	72·60	36·25	162	$6{\cdot}92 \times 10^6$	4·9–5·7	0·12–0·13
25	73·00	36·25	162	$6{\cdot}98 \times 10^6$	4·6–5.6	0·11–0·13
26	67·80	40·6	170	$7{\cdot}64 \times 10^6$	3·8–5·0	0·095–0·12
27	81·40	36·25	180	$8{\cdot}61 \times 10^6$	2·8–4·2	0·059–0·088
28	81·15	38·75	192	$9{\cdot}78 \times 10^6$	3·7–4·3	0·078–0·091
29	81·30	41·25	205	$11{\cdot}1 \times 10^6$	3·2–4·0	0·067–0·084
30	73·95	60·6	275	$20{\cdot}0 \times 10^6$	1·9	0·044

† The Taylor number is defined as

$$T = \frac{4(R_2 - R_1)^4 (\omega_1 R_1)^2}{(R_2^2 - R_1^2)\,\nu^2}.$$

TABLE 1. Experimental results

analysis of the systematic errors which might have been incurred during the test has been carried out by Kirchner (1968). Essentially, the analysis shows that the systematic errors are small compared with the uncertainties in the critical time determination.

The average spacing (Z) between the instability disks was scaled from the motion pictures using a known reference length in the vertical direction, and is shown as a function of Reynolds number in figure 6. The general decrease in Z with increasing Reynolds number is quite evident. The steady-state instability spacing is also shown in figure 6. It is seen that the spacing for the time-dependent case is significantly smaller than the steady-state spacing.

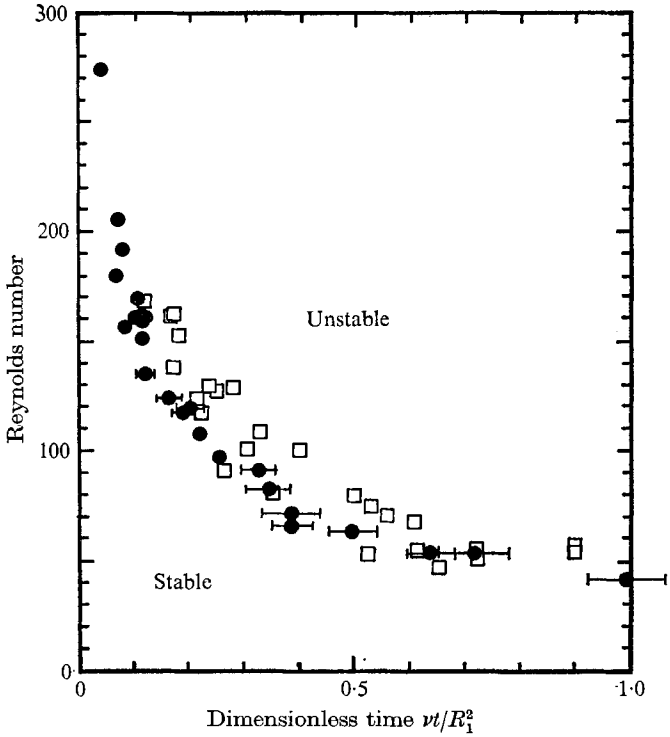

FIGURE 5. Experimental results (Reynolds number *versus* dimensionless critical time τ): ●, present experiment; □, Chen & Christensen (1967).

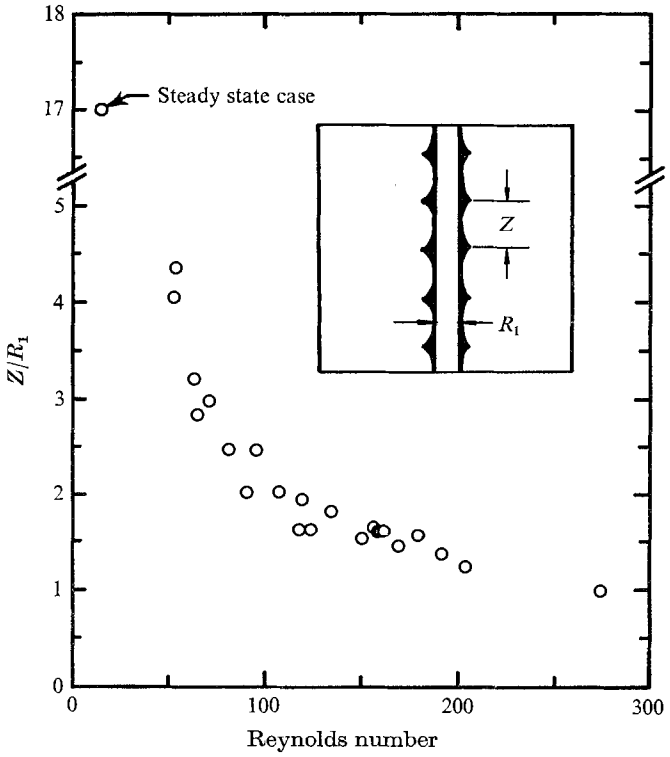

FIGURE 6. Average dimensionless disk spacing *versus* Reynolds number.

4. Conclusion

In this investigation we have attempted to provide reliable experimental data on the instability of the time-dependent laminar flow of a viscous incompressible fluid between concentric rotating cylinders, against which theoretical predictions may be compared. These results were for the wide-gap case with radius ratio of 0·1 and a stationary outer cylinder. Both the critical time and the average spacing between the instability disks have been experimentally determined. The results indicate that the marginal stability curve (figure 5) is not significantly dependent on the gap-width of the cylinders, provided it is large.

This research has been supported by the National Science Foundation under grants GK-1269 and GK-2096. R.P.K. gratefully acknowledges financial aid by NASA (Predoctoral Traineeship) and the Ford Foundation.

REFERENCES

CHEN, C. F. & CHRISTENSEN, D. K. 1967 Stability of flow induced by an impulsively started rotating cylinder. *Phys. Fluids*, **10**, 1845.

CHRISTENSEN, D. K. 1966 The stability of non-steady rotational fluid flow. M.S. Thesis, Dept. of Mech. and Aero. Engr., Rutgers University (TR 111-ME-F).

DONNELLY, R. J. 1964 Experiments on the stability of viscous flow between rotating cylinders. III. Enhancement of stability by modulation. *Proc. Roy. Soc.* A **281**, 130.

KIRCHNER, R. P. 1968 The stability of viscous time-dependent flow between concentric rotating cylinders with a wide gap. Ph.D. Thesis, Dept. of Mech. and Aero. Engr., Rutgers University (TR 121-MAE-F).

TAYLOR, G. I. 1923 Stability of a viscous liquid contained between two rotating cylinders. *Phil. Trans.* A **223**, 289.

WALOWIT, J., TSAO, S. & DIPRIMA, R. C. 1964 Stability of flow between arbitrarily spaced concentric surfaces including the effect of a radial temperature gradient. *J. Appl. Mech.* **31**, 585.

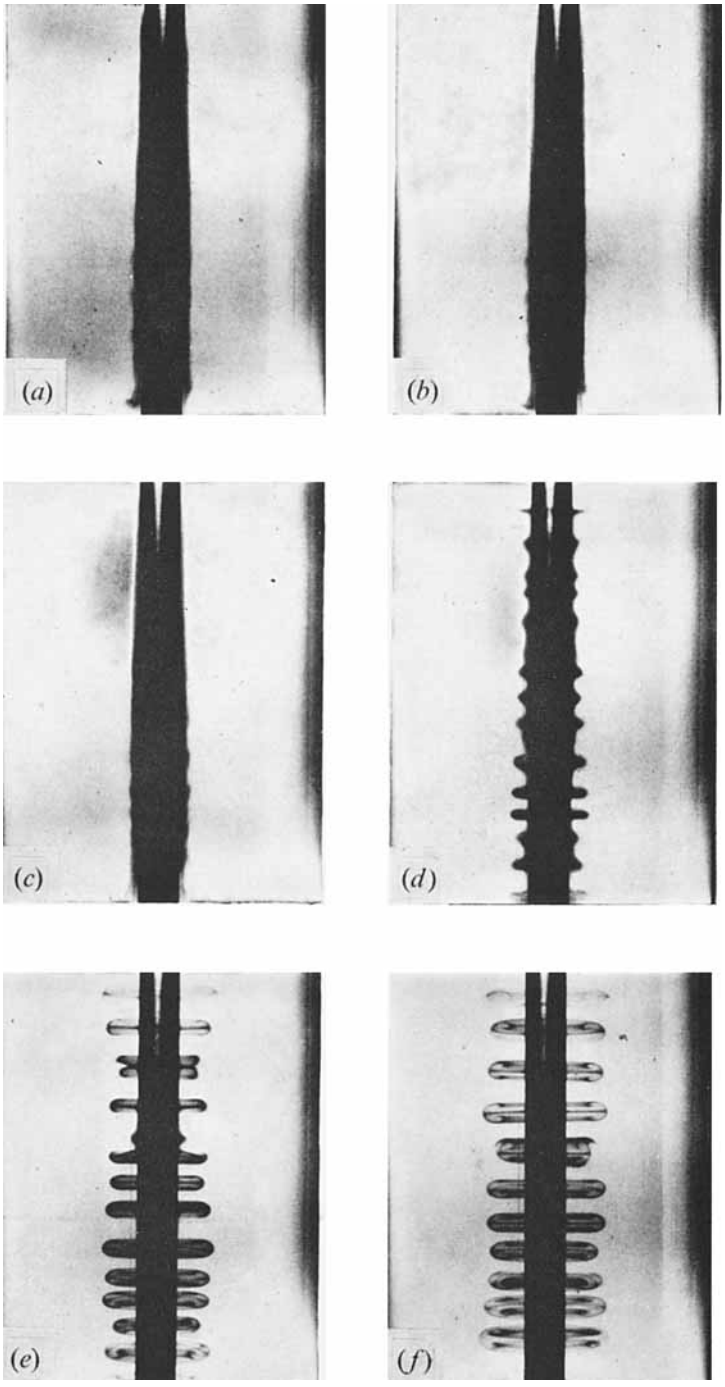

FIGURE 2. Growth of time-dependent Taylor instabilities at 26·9 r.p.m.: (*a*) dye injection before impulsive start; (*b*) laminar diffusion of dye before onset of instability, $t = 4{\cdot}1$ sec; (*c*) start of instability, 8·0 sec; (*d*) instability disks, 12·8 sec; (*e*) toroidal vortices, 17·8 sec; (*f*) toroidal vortices, 25·6 r.p.m., 20·2 sec.

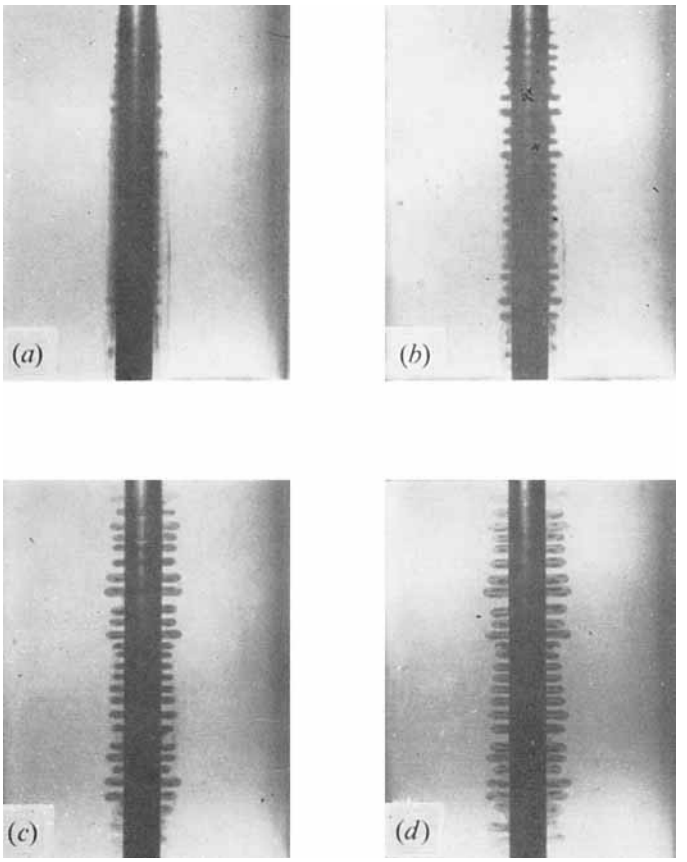

FIGURE 3. Growth of time-dependent Taylor instabilities at 60·6 r.p.m. (critical time = 1·9 sec): (*a*) t = 3·2 sec; (*b*) 3·9 sec; (*c*) 4·6 sec; (*d*) 5·3 sec.